

MUSASHINO UNIVERSITY SCHOOL GYMNASIUM: DESIGN AND TESTING OF A TIMBER-STEEL HYBRID BEAM STRING STRUCTURE

Nicolas Giron¹, Hiroaki Harada²

ABSTRACT: This paper discusses the design and construction of the gymnasium at Musashino University's Musashino Campus in Tokyo, Japan. The project integrates a hybrid section combining steel and European redwood, addressing the need to blend the building harmoniously with the campus's lush greenery. A key design challenge was to incorporate wood as a significant structural element while adhering to Japan's stringent fire regulations. The solution involved a T-shaped steel section with a timber sandwich, preventing steel web buckling and achieving superior structural performance. Approximately 50 cubic meters of timber were used, enhancing both the aesthetic appeal and the environmental sustainability of the project. The hybrid approach allowed the beam string structure to meet design load requirements effectively. Full-scale testing confirmed the structural integrity and load-bearing capacity of the hybrid section, matching those of a full steel section.

KEYWORDS: Beam-string structure, Timber-steel hybrid, T-shaped section, Long span, Buckling

1 – INTRODUCTION

A beam-string structure incorporating a hybrid timber-steel section is proposed to support the 28 meters span roof of the Musashino University Gymnasium. This hybrid section features a T-shaped steel component that is susceptible to buckling, combined with two rectangular timber sections. This paper details the design of each element of the hybrid configuration, along with the results of computational analysis and full-scale testing.

2– BACKGROUND

The Musashino Campus of Musashino University, located in Tokyo, Japan, boasts a rich landscape adorned with numerous trees, including the iconic Japanese cherry blossoms. When the project to rebuild the old gymnasium commenced, it became clear that the design should harmonize with the campus's natural greenery by incorporating wood. The goal was to use wood not only



Figure 1. Gymnasium outside and inside.

¹ Nicolas Giron, Engineering Department (Structural Design Section), NIKKEN SEKKEI LTD, Tokyo, Japan, giron.nicolas@nikken.jp

² Hiroaki Harada, Engineering Department (Structural Design Section), NIKKEN SEKKEI LTD, Tokyo, Japan, haradah@nikken.jp

as a finishing material but also as a structural element within the string beam system that supports the gymnasium roof. However, Japan's stringent fire regulations posed challenges for using timber as a structural component. To overcome these limitations, a combination of timber and steel was employed, leveraging the strengths of both materials while mitigating their respective weaknesses. The resulting space beautifully showcases the aesthetic appeal of wood, as depicted in Fig. 1 along with the building outside.

3 – PROJECT DESCRIPTION

3.1 ARCHITECTURAL OUTLINE

The gymnasium is a two-story mixed-use structure with an underground level, reaching a height of 15 meters and encompassing a total floor area of 3,400 square meters. Its footprint measures approximately 28 by 61 meters. In addition to the main arena, which spans 28 by 36 meters, the facility includes dedicated spaces for kendo and gymnastics, along with essential amenities.

To minimize the building's environmental impact throughout its lifecycle, an underground trench system combined with eco-walls has been implemented. During the summer, outside air is drawn into the underground trench, where it is cooled before being circulated into the building. In the winter, the air beneath the roof is warmed by sunlight and then introduced into the interior. This innovative design effectively reduces electrical consumption for air conditioning, promoting energy efficiency.

3.2 STRUCTURAL OUTLINE

Apart from the arena, the gymnasium is constructed using reinforced concrete with shear-bearing walls and features a spread foundation. The arena roof is supported by tree-like steel columns, each standing 10 meters tall and spaced 7.2 meters apart. These columns consist of two steel pipes connected by a steel web, providing ample space for the eco-walls while ensuring sufficient strength and stiffness to withstand lateral loads caused by wind and earthquakes.

At the top of each column "trunk," four "branches" extend outward, supporting the beam string structure of the roof, which spans 28 meters with a rise of 2.5 meters. The adoption of the string-beam structure offers excellent structural performance while minimizing its impact on the interior space. The lower chord is a tensioned steel string, resulting in a compact profile. The design of the beam string structure is illustrated in Fig. 2.

During the initial design phase, both the arch beam and the struts were considered for construction using timber. However, due to Japan's stringent fire regulations and the client's requirements, a hybrid solution combining steel and European redwood was ultimately selected. Approximately 50 cubic meters of timber were utilized in this project.

4 – DESIGN PROCESS

4.1 STRING-BEAM STRUCTURE

The roof of the gymnasium is constructed with galvalume steel plates, and when combined with the ceiling, wood, and other finishing materials, it accounts for a superimposed dead load of 800 N/m², along with a live load of 600 N/m² (which is considered to be 0 N/m² in the event of an earthquake). Additionally, the self-weight of the structure is approximately 600 N/m², resulting in a total vertical load of $w = 2,000$ N/m².

For lateral load considerations, a horizontal acceleration of 9.8 m/s² is taken into account, leading to a lateral load of 1,400 N/m². The roof area measures approximately 1,550 m², and the rise of the string-beam structure is $h = 2.5$ meters.

Vertical load design

To effectively resist vertical loads such as gravity, snow, and upward wind loads over a span of 32 meters, a string-beam structure has been adopted. The beams are spaced at intervals of $b = 3.6$ meters. The upper chord features an arch shape, and three struts are strategically placed along the string-beam structure to reduce bending moments.

The inner span between the branches measures $l = 21.2$ meters. The anticipated axial force in the bottom chords is calculated as N_{Ci} in (1). To control structural deflection, a

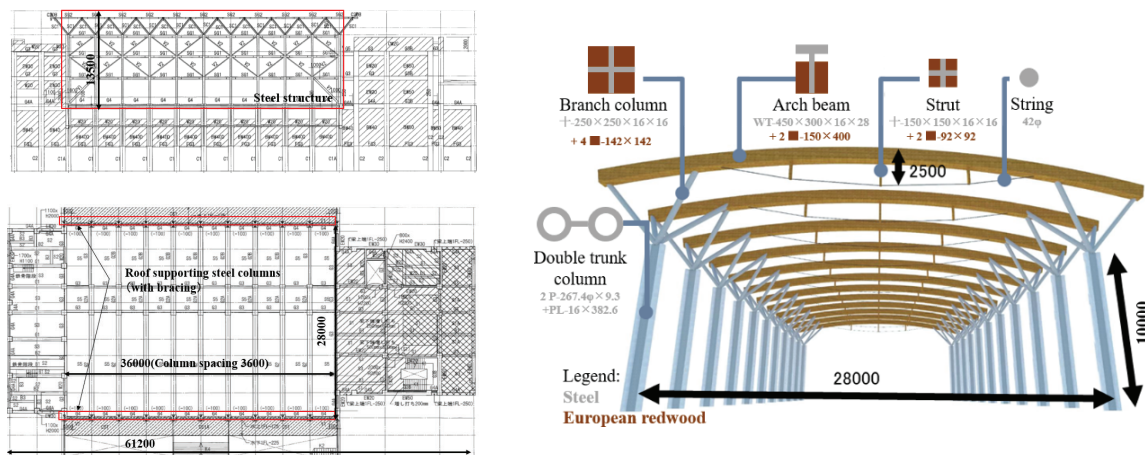


Figure 2. Upper left: Elevation. Lower left: Floor plan. Right: Roof structure system diagram.

strain of approximately 100 N/mm² is established, leading to the selection of a 42 mm diameter steel rod for the string. For the arch beam, the thrust applied by the inclined branches must be considered, resulting in an additional compression thrust leading to a maximum compression strength of 186 kN. Additionally, the arch beam must support a bending moment M calculated in (2). The displacement, axial force, and bending moment diagrams are illustrated in Figs. 3, 4, and 5.

$$N_{Ch} = 1/8 \times w \times b \times l^2 / h = 1/8 \times 2.0 \times 3.6 \times 21.2^2 / 2.5 = 162 \text{ kN} \quad (1)$$

$$M = 1/8 \times w \times b \times (l/4)^2 = 1/8 \times 2.0 \times 3.6 \times 5.3^2 = 25 \text{ kNm} \quad (2)$$

For a string-beam structure to function effectively, it is essential that the anchor points can move horizontally to allow for axial force development. Typically, one anchor point is designed to slide horizontally due to the structure's self-weight or additional preloading. Once this point has slid, the other anchor points remain fixed to support lateral loads from earthquakes or wind. In this particular building, however, the reduced lateral stiffness of the trunk columns supporting the roof allowed for sufficient lateral displacement at the top of each column due to the structure's self-weight, aligning with the expected axial forces at the design stage. Furthermore, the columns were inclined so that they would become vertical once the roof-induced lateral displacement occurred.

Lateral load design

As mentioned in the previous section, the stiffness of the trunk columns is limited. Consequently, the roof is equipped with bracing to ensure that, in the event of an earthquake or strong wind acting in the direction of the string beam, the lateral loads are effectively transferred to the reinforced concrete walls at both ends of the roof. The total inertia of the roof is approximately calculated. In the case of lateral loads acting in the cross direction, vertical bracing is installed between the trunk columns to transfer the roof's lateral load down to the ground floor. To ensure the integrity of the roof structure, 36 mm diameter rods

are designed to withstand this load. Additional details and explanations can be found in Fig. 6.

4.2 HYBRID SECTION

Concept

To maximize the visibility of timber in the roof structure, a T-shaped section was selected for the steel component of the chord beam. As discussed in the previous section, this T-shaped section experiences both compressive axial forces and bending moments. Throughout most of the section, the bending moment induces tension in the web of the section; however, at the connections with the branches, compression occurs, which increases the risk of buckling in the web.

To address this risk, the web plate is sandwiched between two pieces of timber, as illustrated in Fig. 7. This hybrid section demonstrates robust structural properties. The thin plates that make up the steel section are strong and stiff but are also susceptible to buckling. In contrast, timber not only provides aesthetic appeal and carbon storage capacity but is also lightweight, allowing for the use of substantial sections that effectively confine the steel web and prevent buckling, as shown in Fig. 8.

The timber is secured to the steel section using 20 mm steel dowels, with a loose hole of 22 mm for the steel. Additionally, a steel cap with a diameter of 40 mm is added to both ends to prevent sliding and enhance confinement. The timber pieces are spaced apart at each beam, resulting in lengths of approximately 2.6 meters. Consequently, no axial force, primary axis shear, or bending moment is expected to occur in the timber section; its primary role is to prevent the buckling of the web in the T-shaped section.

The T-section utilized in this project has a height of 450 mm and a web thickness of 16 mm. According to Japanese standards, the effective width for a steel plate in a T-section is calculated as 13.2 times the plate thickness,

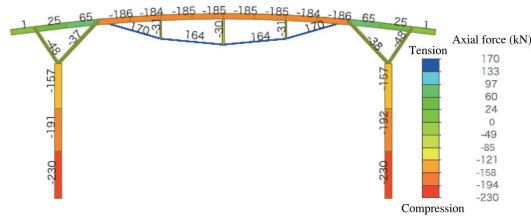


Figure 3. Gravity load axial force diagram.

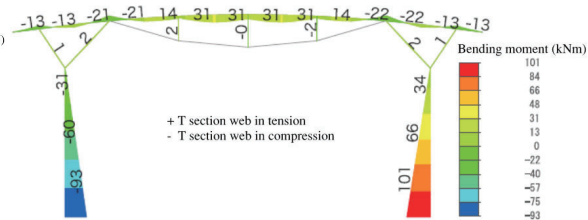


Figure 4. Gravity load bending moment diagram.

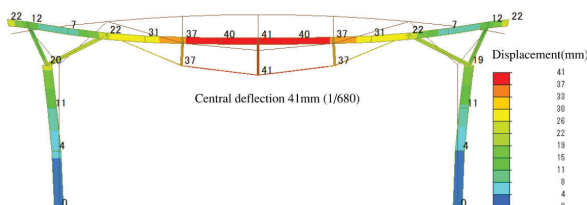


Figure 5. Gravity load displacement diagram.

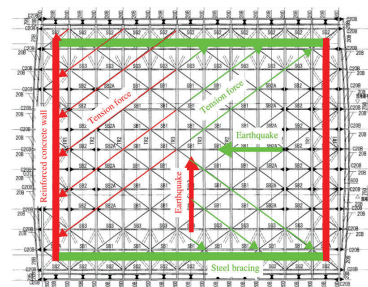
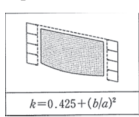
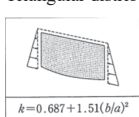
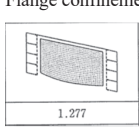


Figure 6. Roof inertia transfer scheme diagram.

resulting in an effective width of 211 mm, which is less than half of the actual height of the section. Consequently, the expected allowable design load and ultimate load for the effective section are, respectively, 4.5 times and 5.0 times smaller than those of the full section, as shown in Table 1.

However, as discussed in the next section, buckling numerical analysis and full-scale testing confirmed that the confinement provided by the timber effectively allows the T-section to support loads equivalent to those of the full steel section.

Table 1: Comparison of allowable/ critical bending moment depending on web buckling type

Buckling type	Effective height mm	Allowable long term bending moment
		Critical bending moment /shear force
 Japanese standard $k=0.425+(b/a)^2$	211	42 kNm (0.22) 122 kNm /114 kN (0.20)
 Triangular distribution $k=0.687+1.51(b/a)^2$	280	74kNm (0.40) 181 kNm /169 kN (0.30)
 Flange confinement 1.277	372	129 kNm (0.69) 329 kNm /306 kN (0.55)
No buckling	450	187 kNm (1.00) 602 kNm /560 kN (1.00)

Structural design (steel section)

To resist the compression and bending moments described in the previous section, a T-section with

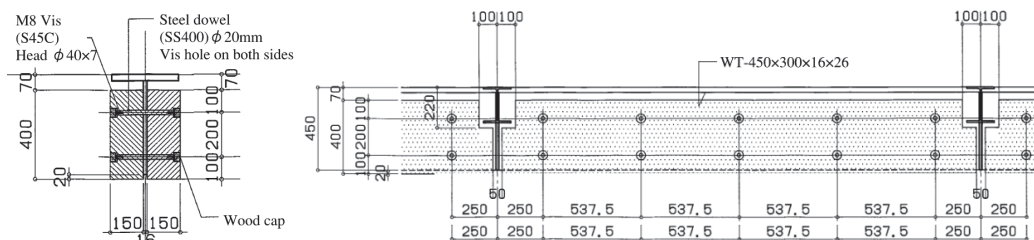


Figure 7. Hybrid section details.

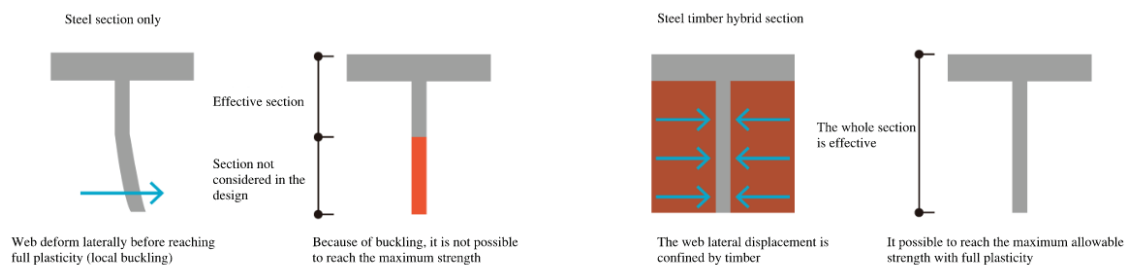


Figure 8. Concept and merits of the hybrid section compared to the steel section.

dimensions 450×300×16×28 mm and a yielding stress of 325 N/mm² has been adopted. Two types of buckling are considered in the design (the buckling of the entire string-beam structure is not addressed in this paper).

The first type is the combination of flexural-torsional buckling due to compressive forces and lateral-torsional buckling due to bending moments affecting the whole section. This is accounted for by reducing the allowable compressive stress f_c and bending stress f_b . The second type of buckling considered is the local plate buckling of the T-web, which is a concern due to its large depth-to-thickness ratio (450/16 = 28). In this case, the allowable strength is calculated by assuming the largest effective section where buckling is unlikely. The design follows the AIJ Recommendations for the Stability Design of Steel Structures. For this grade of steel, the maximum ratio is 13.2, leading to an effective cross-section of T-211×300×16×28 mm.

For the studied beam under long-term vertical loads, the allowable compressive stress is $f_c = 189\text{N/mm}^2$ and the bending stress is $f_b = 213\text{N/mm}^2$. The cross-section area is $A = 152\text{cm}^2$ and the resistance moment about the neutral axis is $W_z = 865\text{cm}^3$. For the effective cross-section, the area is $A_e = 114\text{cm}^2$ and the effective resistance moment is $W_{ze} = 193\text{cm}^3$.

The demand-to-capacity ratios for the two cases are R_1 and R_2 as in (3) and (4) respectively.

The demand-to-capacity ratio is three times larger for local buckling; therefore, confining the web to prevent local buckling, is the most effective strategy to enhance structural performance.

$$R_1 = N/(f_c \times A) + M/(f_b \times W_z) = 186/(152 \times 189/10) + 21/(213 \times 865/1000) = 0.06 + 0.11 = 0.17 \quad (3)$$

$$R_2 = N/(f_c \times A_e) + M/(f_b \times W_{ze}) = 186/(217 \times 114/10) + 21/(217 \times 193/1000) = 0.08 + 0.50 = 0.58 \quad (4)$$

Structural design (timber section)

To determine the expected minimum required timber cross-section for effective confinement, we refer to the Japanese Design Standard for Steel Structures - Based on Allowable Stress Concept -. According to this standard, the minimum confinement stiffness K_{min} should be four times the axial strength of the confined section N' divided by the spacing of the confinement l_b . Additionally, the section must be capable of bearing 2% of the axial force N' with a corresponding bending moment M_b , calculated as in (5) and (6) respectively. The expected force diagram is illustrated in Fig. 9.

For instance, in the case of four connections, the confinement spacing is $l_b=717\text{mm}$, and each connection covers a height of approximately 200 mm of steel. Also, for the considered timber section, a cross-section of $200\times 150\text{ mm}$ is used, with a Young's modulus $E=10,500\text{N/mm}^2$, and an allowable bending stress of $f_b'=14.4\text{N/mm}^2$. Considering a yielding stress for the web of $f_w=396\text{N/mm}^2$, the required stiffness can be calculated in (7). Also, for a supported simple beam with a concentrated load at the center, the stiffness K is given by the formula in (8). In (9) the allowable bending moment is calculated. Hereafter, I' is the second moment of area and Z' is the section modulus of the timber cross-section.

$$N' = A' \times f_w = 16 \times 200 \times 396 = 127 \text{ kN} \quad (5)$$

$$M_b = N' \times 2/100 \times l_b/4 = 127 \times 2/100 \times 717/4 = 4.5 \text{ kNm} \quad (6)$$

$$K_{min} = 4 \times N'/l_b = 4 \times 127/717 = 7 \text{ kN/mm} \quad (7)$$

$$K = 48 \times E \times I'/l_b^3 = 48 \times 10.5 \times 56,250/717^3 = 77 \text{ kN/mm} \quad (8)$$

$$M_a = f_b' \times Z' = 14.4 \times 750 = 10.8 \text{ kNm} \quad (9)$$

The timber satisfies the standard requirements with a considerable safety margin. Therefore, it is expected that the maximum bending capacity of the T-section can be reached before buckling occurs.

However, as discussed in the following section, a stiffness greater than five times K_{min} is necessary to ensure proper confinement. The evaluation of K does not account for shear stiffness or the stiffness of the connections; thus, when designing the timber, a thorough evaluation of stiffness or an adequate margin in stiffness should be considered. Also, for the bending moment and lateral force, the computed analysis values are 0.25 kNm and 2.6 kN, which are significantly smaller than the theoretical values.

4.3 – PERFORMANCE ASSESSMENT

To evaluate the confinement performance of the timber in restraining web buckling, the testing setup depicted in Fig. 10 is employed. This setup enables uniform compression loading on the steel web over a large interval. Three variations of the setup are tested, Type A: only steel, Type B: A hybrid section with four connections between timber and steel (pitch = 716.7 mm), Type C: A hybrid section with five connections (pitch = 537.5 mm).

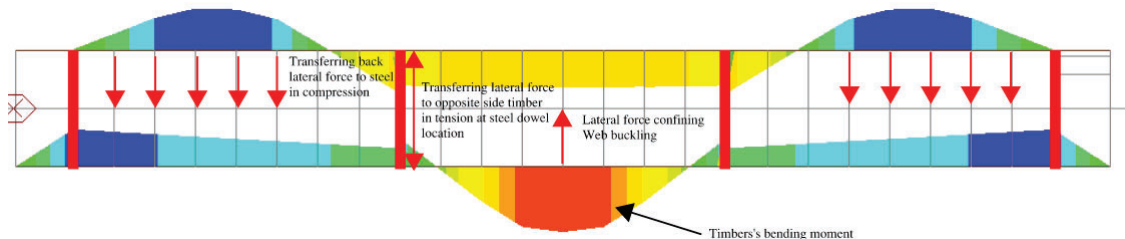


Figure 9. Conceptual diagram of the confinement mechanism of the web by timber.

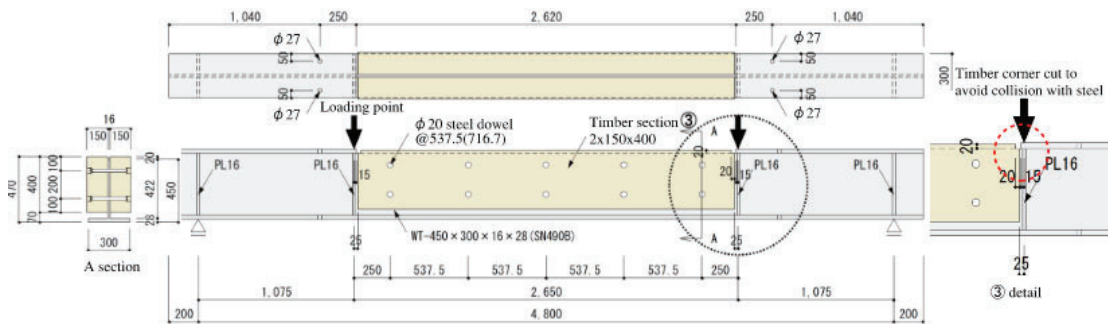


Figure 10. Testing setup of the performance assessment.

Each of these setups is replicated using a finite element analysis model for comparative purposes. According to the inspection certificate for the steel used in the full-scale testing, the yielding stress for the web is 396 N/mm², while the yielding stress for the flange is 361 N/mm². These same values are utilized in the computational analysis model and for theoretical value calculations.

Computational analysis: Computational model

A finite element model has been developed using two-dimensional plate elements to represent the steel section and beam elements for the confining timber and steel dowels. This model accurately simulates the experimental setup.

At the dowel connections between the steel and timber, axial forces are transferred in both tension and compression. In contrast, between the steel web and the

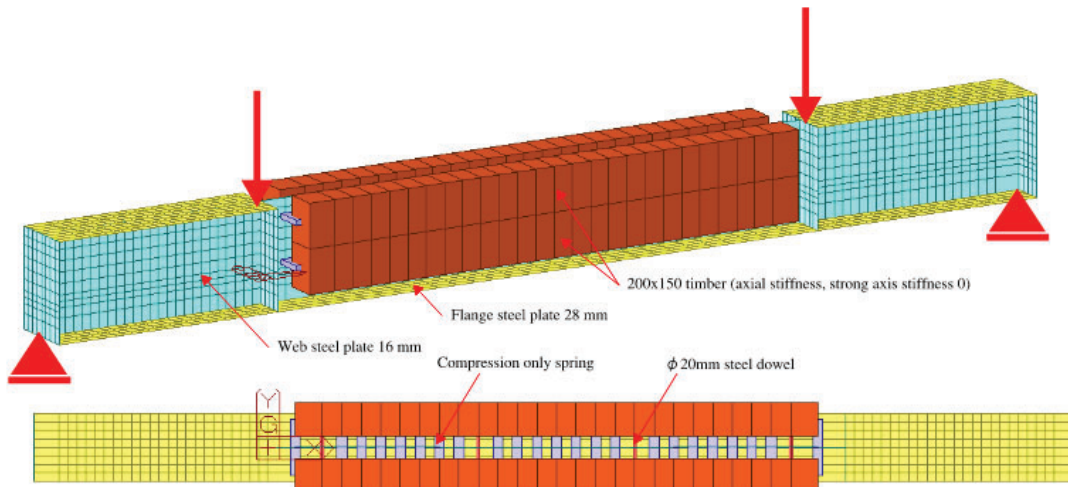


Figure 11. Computational analysis model of the hybrid section.

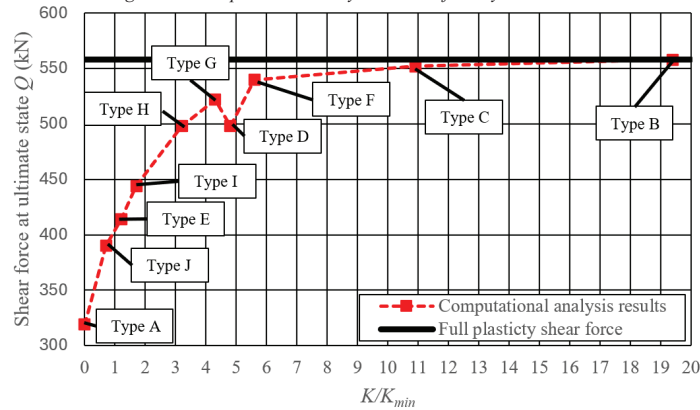


Figure 12. Computational analysis results, relation between confining stiffness and ultimate capacity

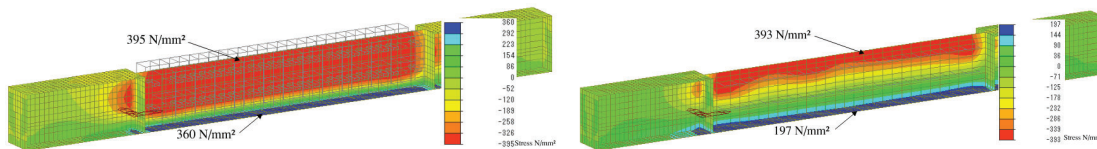


Figure 13. Stress distribution at ultimate state for Type C (left) and Type D (right).

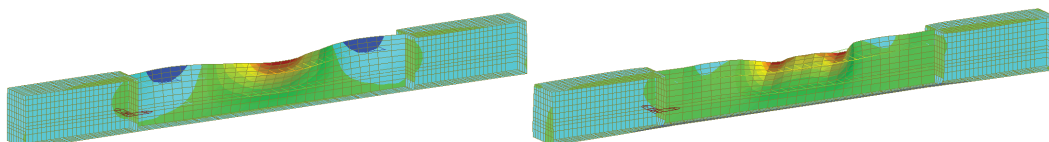


Figure 14. Buckled shape at ultimate state for Type G (left) and Type D (right).

timber, only compressive forces are transmitted. The computational model is illustrated in Fig. 11. This approach allows for a comprehensive analysis of the interactions between the materials and the effectiveness of the confinement in preventing web buckling.

Computational analysis: Analysis

First, a buckling analysis is performed to determine the mode shape of the buckled T-shaped steel cross-section and to identify the critical buckling load. Following this, the steel shape is deformed to align with the mode shape, resulting in a maximum deformation of $450/1000 = 0.45$ mm.

Next, a nonlinear model is applied to the steel elements, and loading is introduced progressively through a pushover analysis. In addition to the original setups (Types A, B, and C), variations with fewer dowels and more slender timber sections are also included in the analysis. This comprehensive approach allows for a thorough investigation of the structural performance under varying conditions and configurations, providing insights into the behaviour of the hybrid system.

Computational analysis: Results

The results of the analysis are summarized in Table 2 and illustrated in Fig. 12. For the types where K/K_{min} is greater than 5, an ultimate bending moment exceeding 95% of the maximum possible value is achieved (specifically for type K), indicating that full plasticity of the steel section has been realized. The type K value of 558 kN demonstrates good agreement with the calculated theoretical value of 560 kN. Therefore, it is concluded

that when K/K_{min} exceeds 5, effective buckling confinement is achieved.

In Fig. 13, a comparison of the stress distribution is presented for type C, which has fully plasticized, and type D, where buckling has occurred. Notably, type D exhibits a smaller stress value compared to the other types, while having an equivalent or larger K/K_{min} ratio. This difference is further explained by the fact that the buckling mode for type D is distinct from that of the other types, as illustrated in Fig. 14, where it is compared to type G, which experiences the same buckling load.

Table 2: Parameters and results of the computational analysis.

Case	Timber thickness	Number of Dowels	Q kN	K/K_{min}	Comment
Type A	-	-	319	0.0	Buckling
Type B	2×150×400	5(@537.5)	558	19.4	Plasticized
Type C	2×150×400	4(@716.7)	552	10.9	Plasticized
Type D	2×150×400	3(@1075)	498	4.8	Buckled
Type E	2×150×400	2(@2150)	414	1.2	Buckled
Type F	2×120×400	4(@716.7)	540	5.6	Plasticized
Type G	2×110×400	4(@716.7)	522	4.3	Buckled
Type H	2×100×400	4(@716.7)	498	3.2	Buckled
Type I	2×80×400	4(@716.7)	444	1.7	Buckled
Type J	2×60×400	4(@716.7)	390	0.7	Buckled
Type K	-	-	558	∞	Pinned



Figure 15. Testing setup overview

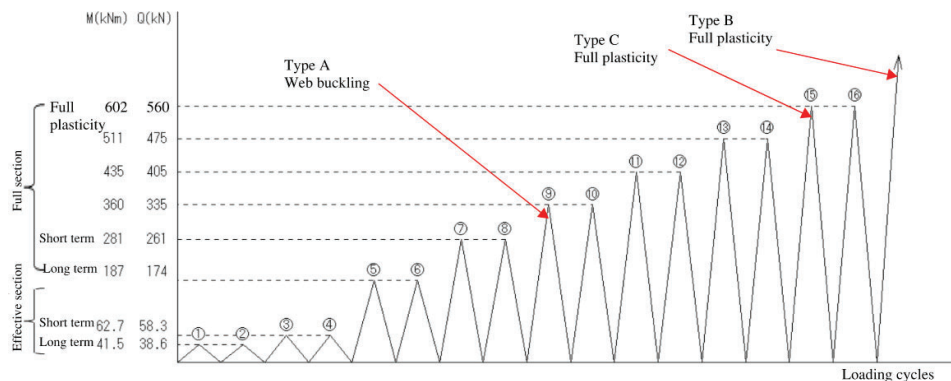


Figure 16. Loading cycles details

Full-scale section strength testing: Setup

The testing setup and loading procedure are depicted in Figs. 15 and 16. The loading steps have been carefully selected to correspond with the various allowable states of both the effective and full sections, enabling appropriate monitoring of potential damage to the timber.

Full-scale section strength testing: Results

For type A, buckling occurred at a load of 344 kN, which is greater than both the theoretical and analytical values. During the testing of type B, it was observed that the clearance between the steel end upper flange and the timber was insufficient, causing the steel plate to push against the timber. This interaction led to an increase in strength to 643 kN, which is 15% higher than the expected maximum value. This outcome did not align with the intended design, prompting the modification for type C by cutting the timber corners to avoid collision.

Despite these adjustments, no damage was reported to the timber except in the areas in contact with the steel and some connections with the steel dowels. For type C, a maximum shear force of 543 kN was achieved, which matched both the theoretical and computational values. However, timber damage was noted at the connection with the steel dowel due to embedding, as shown in Fig. 17. No other damage was reported for the timber; but after dismantling the test specimen, some bending of the steel dowels was observed, as illustrated in Fig. 18. The ultimate state of each test is depicted in Fig. 19.

Although some damage was reported, it occurred during the final loading cycle, and therefore, no damage is anticipated for the timber throughout the building's lifecycle. Initially, the building was designed with type B

connections (5 sets of dowels); however, based on the results of the computational analysis and full-scale testing, the design was modified to type C connections (4 sets of dowels).

5 – RESULTS

The study yielded several significant outcomes, with the most notable being the effective prevention of buckling in the steel web, achieved through the confinement provided by the timber components. The hybrid timber-steel section demonstrated robust structural characteristics, as validated by both numerical analyses and full-scale testing. These results confirmed the initial design hypothesis, illustrating that the hybrid solution can achieve the same load-bearing capacity as a full steel section. This finding underscores the potential of hybrid designs to enhance structural performance while capitalizing on the aesthetic and environmental benefits of timber.

The experimental program provided compelling evidence regarding the performance of the hybrid section. The successful mitigation of buckling in the steel web was primarily attributed to the effective confinement from the timber components. This was substantiated through a combination of numerical simulations and full-scale testing, which collectively demonstrated that the hybrid section maintained its structural integrity under



Figure 17. Embedding of timber at connection with the dowel.



Figure 18. Dowels state of type B testing.

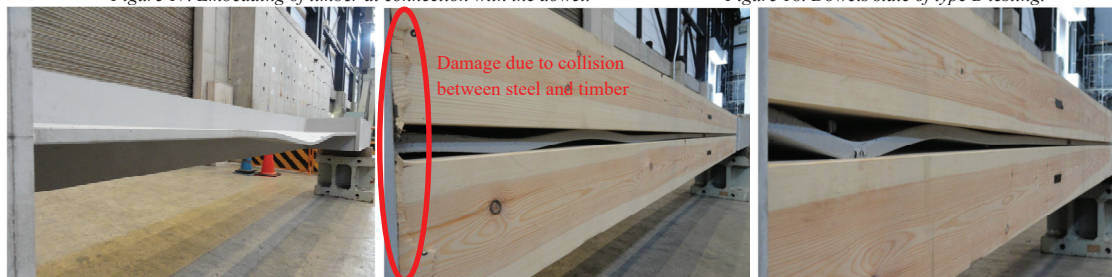


Figure 19. From left to right, ultimate state of testing type A, B and C

bending while the web was in compression, even after yielding.

Analysis revealed that theoretical predictions for buckling loads were generally conservative when compared to experimental results. Although slight discrepancies in the required stiffness and strength parameters for buckling confinement were noted, these could be addressed with sufficient design margins or detailed calculations, facilitating the structural design of an efficient timber section.

While minor damage to the timber was observed—primarily in localized areas around the connections during the final loading phase—this damage was minimal and did not compromise the structural integrity or aesthetic appeal of the timber. This suggests that the hybrid section is both durable and suitable for long-term use in construction applications. Furthermore, the results highlighted that the proposed hybrid solution achieved a significant increase in design capacity, extending the load-bearing range while preserving aesthetic qualities and sustainability benefits. To mitigate potential damage to the timber, the bolt hole located near the free edge of the web could be elongated in the axial direction, effectively reducing the timber's contribution to the bending of the hybrid section.

6 – CONCLUSION

The proposed hybrid timber-steel section was successfully utilized to construct the arch beam of the string-beam structure supporting the roof of Musashino University Gymnasium. Initially designed based on established standards and numerical analysis, the section was validated through full-scale testing. This approach allowed for a nearly invisible steel structure, resulting in a spacious interior enhanced by the warmth of wood, as illustrated in Figures 21, 22, and 23, which depict the roof during construction and after completion.

The incorporation of timber not only enhances the aesthetics of the main arena and provides essential carbon storage—an increasingly critical issue in today's environmental context—but also improves the structural properties of the embedded steel section. The hybrid timber-steel section extended the design range by 350% and increased the ultimate strength capacity by 50%, as shown in Fig. 20.

The design methodology was articulated with concrete examples, demonstrating a strong alignment between computational analysis and full-scale testing. This validation suggests that future designs could rely primarily on computational analysis to determine appropriate timber cross-sections.

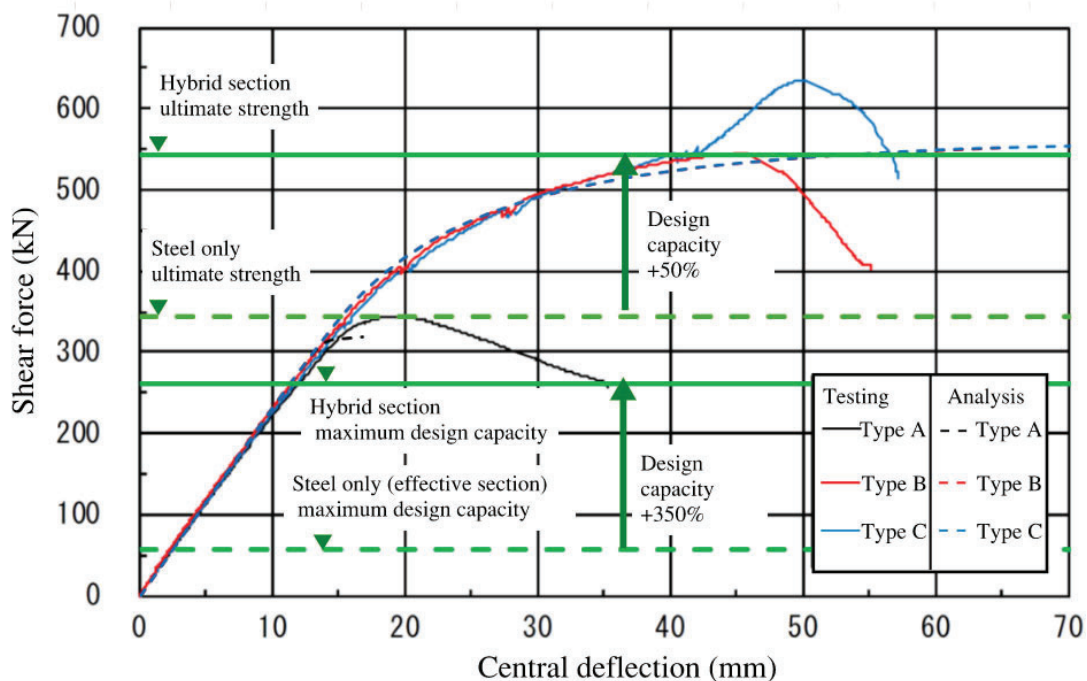


Figure 20. Analysis and testing results.

While minor damage was observed during testing, it was limited to specific areas and occurred only during the final loading cycle. This indicates that the timber components are likely to maintain their integrity throughout the building's lifecycle. Additionally, improvements to the connections between timber and steel could be proposed to address this issue.

Future research is recommended to further explore the performance of hybrid timber-steel systems under a broader range of loading conditions, including axial forces and combinations with bending. Moreover,

designs that allow timber to contribute to both stiffness and load-bearing capacity should be considered, with special attention given to potential damage to timber and the design of connections.

7 – REFERENCES

- [1] H. Harada, N. Giron, T. Aoyama, and S. Takezaki. "Experimental Study on Ultimate Strength of Beam with Wood and Steel" In: AIJ Summaries of technical papers of annual meeting (2017), pp. 1475–1476. (in Japanese)



Figure 21. Roof during construction



Figure 22. Connection between the string and the strut



Figure 23. Inside of the gymnasium